



2DH numerical simulation of ice dynamic during break up

Ali Oveysy^{1,2}, Yonas B. Dibike², Terry D. Prowse², Spyros Beltaos³, and Erik de Goede⁴

¹*Hydrotechnical Engineer, Tetra Tech EBA, Water and Marine Engineering, Vancouver, BC, Canada (aoveisyq@gmail.com)*

²*Environment Canada / Water & Climate Impacts Research Centre (W-CIRC), University of Victoria, Victoria, BC, V8W 3R4, Canada*

³*Watershed Hydrology and Ecology Research Division, National Water Research Institute, Environment Canada, 867 Lakeshore Rd., Burlington, ON L7R 4A6*

⁴*Deltares, Software Centre, Delft, Boussinesqweg 1, 2629 HV Delft, Netherlands*

Rivers in mid to high-latitude regions experience periods of ice cover and subsequent breakups. During the breakup period, the transport of ice parcels is very dynamic and the movement of ice, with the potential for ice jam and subsequent release, change the hydraulics and transport regimes in these rivers. The significant increase in water level during ice jams may cause inundation threats to nearby communities, and accelerate sediment transport and erosion. These make the study of the ice breakup an essential part of cold region hydraulics. Numerical models have been powerful and reliable tools for predicting the river flow characteristics in the past decades and recently several efforts have been made to include river ice dynamics in the models. Here we developed a river ice dynamic model using a discrete parcel scheme that mitigates the problem based on Moving Particle Semi-implicit Method (MPS) with a visco-plastic rheology. The model is two-way coupled with a widely used open source hydrodynamic and transport model called Delft3D (oss.deltares.nl). The new modelling approach was verified against theory and applied to Thames River, ON, Canada. In this paper we focus more on adaptation of the MPS method in modelling ice dynamics in rivers.

1. Introduction

The ice transport in rivers has similar basics as the ice transport in sea and lakes (Hibler, 1979; Wake and Rumer, 1983), however the usual conventional Eulerian approach results in high numerical diffusivity and dispersion. Other approaches such as the adaptive grid scheme, which uses Lagrangian grid cells to reduce diffusivity at the edge of the ice (Pritchard et al., 1990) are not accurate in the ice domain and lose accuracy in the river when the ice edge deformation is high. Particle-in-cell (Flato, 1993) is another method which performs better [Harlow, 1964] in more dynamic ice transport mode, but the several interpolations from/to particles and Eulerian grid introduce significant diffusivity. The fully Lagrangian mesh free method has been used in recent research. Dorsk (2006) has used a discrete element method to model ice parcels as circular ice particles that interact with each other and boundary walls. However, they were not successful in modeling of ice ridges properly. Lindsay and Stern (2004) used SPH (Smoothed Particle Hydrodynamics) for modelling sea ice and divided domain to Lagrangian cells then for the calculation of the strain rate determined the spatial derivatives of the velocity by a weighted summation of the velocities of adjacent cells. The force balance equation is solved for each dynamic cell with standard wind and water stress terms, a Coriolis term, and an internal ice stress term. Shen et al (2000) used SPH for ice transport in rivers with a viscous-plastic model for ice. He later validated his model for ice thickness in Thames River (Shen et al., 2008). Nolin et al. (2009) have coupled a 1D finite volume hydrodynamics model of the Saint-Venant equations model known as KIMBULA (Roubtsova and Kahawita, 2009) with a 2D SPH ice transport model smoothed particle ice dynamics equations for rivers (SPIDER).

Here we developed a river ice dynamic model using Moving Particle Semi-implicit Method (MPS). The model is coupled with Delft3D a widely used hydrodynamic and transport model. The model was verified against theory and applied in the case of Thames River, ON, Canada to ensure the applicability of model in real case.

2. Method

With the consideration of ice as a continuum the governing equations for conservation of momentum in two-dimensional horizontal plane is as follows.

$$MDV_{ice} / Dt = F_w + F_a + F_{ice} + F_g \quad [1]$$

Where $M = \rho_{ice} t_{ice} N$ is ice mass per unit area, ρ_{ice} , t_{ice} , N are ice density, ice thickness, and ice concentration respectively. F_w and F_a are water and air stress terms respectively. F_{ice} is ice internal resistance and F_g is the gravitational force due to the slope of the water surface. These forces are defined as follow,

$$F_w = N \rho_w c_w |V_w - V_{ice}| (V_w - V_{ice}) \quad [2]$$

$$F_a = N \rho_a c_a |V_a - V_{ice}| (V_a - V_{ice}) \quad [3]$$

$$F_g = -Mg \nabla \xi \quad [4]$$

V_{ice} , V_w , V_a are the ice velocity, water velocity and wind velocity respectively. g is the gravitational acceleration and ξ is the water surface elevation. ρ_a , ρ_w , c_w , c_a are density of air, density of water, water-ice drag and air-ice drag coefficient respectively.

Constitutive law is a viscous-plastic model with elliptic yield curve (Wake and Rumer , 1983; Hibler, 1979).

$$\sigma_{ij} = 2\vartheta \dot{\epsilon}_{ij} + (\zeta - \vartheta) \dot{\epsilon}_k \delta_{ij} - P \delta_{ij} / 2 \quad [5]$$

$$\Delta^2 = (\dot{\epsilon}_{xx} + \dot{\epsilon}_{yy})^2 + [(\dot{\epsilon}_{xx} - \dot{\epsilon}_{yy})^2 + 4\dot{\epsilon}_{xy}^2] / e^2 \quad [6]$$

$$\dot{\epsilon}_{xx} = \frac{\partial u}{\partial x}, \dot{\epsilon}_{yy} = \frac{\partial v}{\partial x}, \dot{\epsilon}_{xy} = \frac{1}{2} \left(\frac{\partial v}{\partial x} + \frac{\partial u}{\partial y} \right) \quad [7]$$

In which $\sigma, \dot{\epsilon}$ are the ice stress and strain rate respectively. $\zeta = \frac{P}{2\Delta}, \vartheta = \zeta / e^2$ are, nonlinear bulk and shear viscosity respectively. u and v are the ice velocities in x and y directions respectively. We defined P as (Shen et al., 1990);

$$P = \tan^2 \left(\frac{\pi}{4} + \frac{\varphi}{2} \right) \left(1 - \frac{\rho_i}{\rho} \right) \frac{\rho_{ice} g t_{ice}}{2} \left(\frac{N}{N_{max}} \right)^J \quad [8]$$

In which φ, N_{max} and J are the ice internal friction angle = 46° , maximum allowable ice concentration and empirical constant respectively =15. In the constitutive law when strain rate goes to very small value the viscosity become large, therefore we limit the ζ, ϑ to minimum of above mentioned Equations and large values. These limiting values are chosen to be large and rarely reached during computation.

3. Implication in MPS

MPS is a Lagrangian mesh free method (Koshizuka and Oka, 1996). MPS uses the weighted average for differential operator for the particles in vicinity of the smoothing length, the weighting function is called kernel function, and unlike SPH there is no gradient of kernel function in this method. In MPS each particle interacts with neighboring particles in vicinity of $R_{ij} < r_e$, R_{ij} is the distance between particles i and j and r_e is the smoothing length in which the particle interacts with other particles, for example $r_e = 3\Delta l$, Δl = is the average distance between the particles. The smoothing function is defined as $W(R_{ij}, r_e) = \left(1 - \frac{R_{ij}}{r_e} \right)^{k=3}$ (Shakibaeinia and Jin, 2010) and used for definition of the physical quantities for example;

$$\left\langle \frac{\partial u}{\partial x} \right\rangle_i = \frac{2}{n} \sum_{j \neq i} \left[\frac{u_j - u_i}{R_{ij}} \frac{x_j - x_i}{R_{ij}} W(R_{ij}, r_e) \right] \quad [9]$$

$$\left\langle \frac{\partial v}{\partial y} \right\rangle_i = \frac{2}{n} \sum_{j \neq i} \left[\frac{v_j - v_i}{R_{ij}} \frac{y_j - y_i}{R_{ij}} W(R_{ij}, r_e) \right] \quad [10]$$

$$\left\langle \frac{\partial v}{\partial x} \right\rangle_i = \frac{2}{n} \sum_{j \neq i} \left[\frac{v_j - v_i}{R_{ij}} \frac{x_j - x_i}{R_{ij}} W(R_{ij}, r_e) \right] \quad [11]$$

$$\left\langle \frac{\partial u}{\partial y} \right\rangle_i = \frac{2}{n} \sum_{j \neq i} \left[\frac{u_j - u_i}{R_{ij}} \frac{y_j - y_i}{R_{ij}} W(R_{ij}, r_e) \right] \quad [12]$$

$$\langle \rho \rangle_i = \frac{\sum_{j \neq i} m_j W(R_{ij}, r_e)}{\int_A W(R_{ij}, r_e) dA} \quad [13]$$

$$\langle n \rangle_i = \sum_{j \neq i} [W(R_{ij}, r_e)] \quad [14]$$

In which m, A, ρ, n are the mass of particles, the effective area, fluid density and density number. These are the components which were needed in the previous section for calculation of internal stresses.

To solve the equation we used Heun's method to calculate ice velocities at t_{n+1} and the leap-frog for calculation of the particles location at t_{n+1} using particle velocities at half time steps. Then the ice properties such as density, and density number will be updated. The ice concentration and thickness of ice is adjusted as the particles change position.

$$N_{t+1} = \frac{\langle \rho \rangle_{t+1}}{\langle \rho \rangle_{i,t}} N_{i,t} \quad , \quad t_{i,t+1} = t_{i,t} \quad \text{if } N_{i,t+1} < N_{max} \quad [15]$$

$$t_{i,t+1} = \frac{N_{i,t+1}}{N_i} t_{i,t} \quad , \quad N_{i,t+1} = N_{max} \quad \text{if } N_{i,t+1} > N_{max} \quad [16]$$

The time steps are limited by

$$\Delta t_i = \beta \min\left(\sqrt{\frac{l_e}{|a_{ice}|}}, \frac{l_e}{|v_{ice}| + C_{ice}}\right) \quad [17]$$

where a_{ice} , C_{ice} and β are the particle acceleration, speed of sound and courant number. The speed of sound depends on the ice properties.

4. Solid boundary condition

The boundary of the river bank and any solid obstacles in the domain are modeled using imaginary particles. For any particle get closer than r_e to the boundary there is an imaginary particle which mirrors the actual particle inside the domain. The mass, pressure, tangential velocity, normal and tangential internal stresses are the same as the real particles and normal velocity and internal shear stresses are in the same magnitude but in opposite direction. The bank friction considered when the particles moves toward the boundary and closer than r_e , then the normal component of the ice stress is calculated and multiplied by a friction coefficient equal to $\tan\varphi$ and acts against the movement.

5. Coupling with Delft3D

The ice advection model was coupled with Delft3D as a hydrodynamic drive of the ice transport. The coupling is two-way, the ice thickness, concentration and velocity are sent to Delft3D and the water velocities and water surface elevation read back from Delft3D. It replaces the ice thicknesses, ice concentrations and ice velocities computed by the ice module of Delft3D (De Goede et al., 2014). The ice depth is subtracted from the water level and the pressure of the ice is added on the water surface. The ice stress on the water is calculated the same as the water stresses on the ice but in opposite direction. This coupling is repeated every specific user define interval, which can be every several hydrodynamic time steps depending on how dynamic is the ice transport.

6. Model verification

We tested the model against the analytical solution of idealized of static ice jam for a rectangular channel with uniform current without bank friction. The thickness of ice can be calculated as;

$$t_i = \left(t_{i0}^2 + \frac{2\rho C_w V_{wx}^2}{\tan^2\left(\frac{\pi+\varphi}{4}\right)\left(1-\frac{\rho_{ice}}{\rho}\right)\rho_{ice}g} x_j \right)^{1/2} \quad [18]$$

In which C_w, V_{wx}, t_{i0}, x_j are ice water drag coefficient, water velocity in x direction and single layer ice thickness and distance from the edge of the ice jam respectively.

For this verification we modeled a rectangular channel with 500 m in width and 5000 m in length with a boom at the downstream end. The ice parcels assumed to be 50x50 m with 0.2 m thickness covering the whole channel with 1000 parcels. C_w, V_{wx}, t_{i0} assumed to be 0.02, 0.6 and 0.2 respectively. Fig. (1) Compares the theory with the model result at different time.

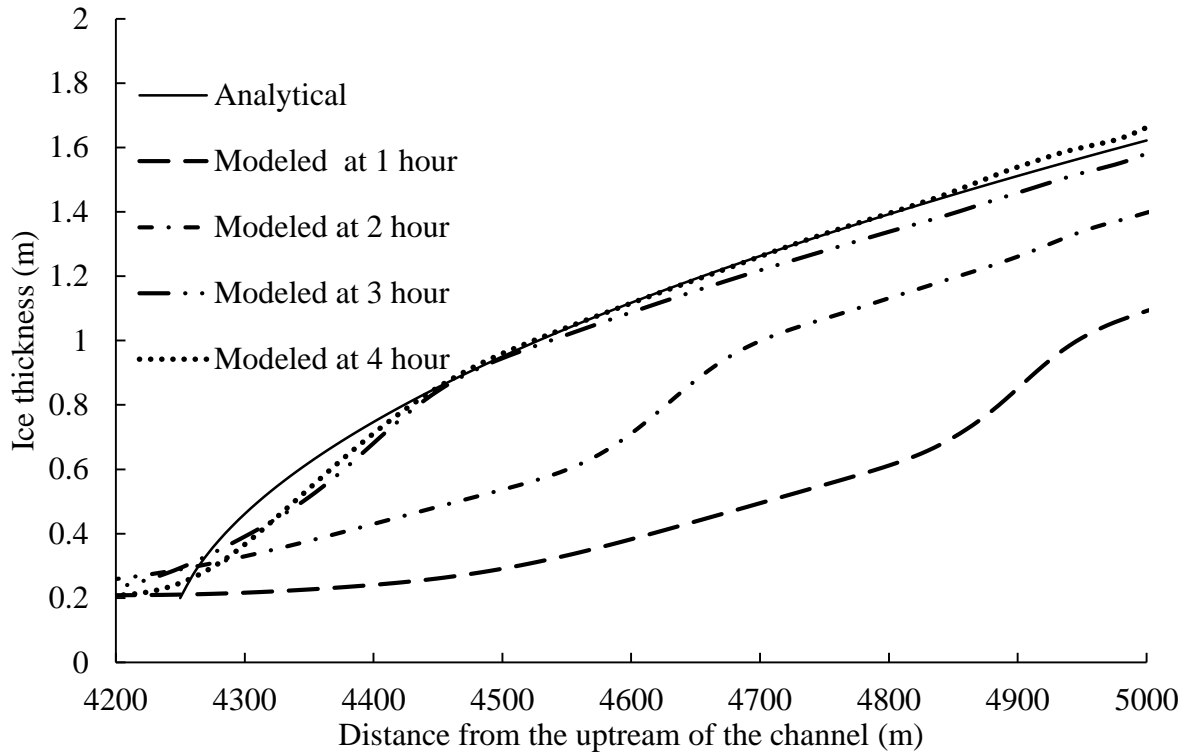


Fig. 1: Comparison of model result with theoretical ice jam in a rectangular channel

7. Formation of ice jam in Thames River, ON

We also setup model and studied the ice jam formation for lower Thames River in southern Ontario, from Chatham to Golf Course for ~11 km with the width of ~100-150 (m). In 1986 there was an ice jam in this river and for the purpose of this study we applied the model for this event to insure the applicability of the model to a prototype case. Fig. 2a shows bathymetry for this part of the river. A constant flow of 290 m³/s was assumed (Beltaos, 1988). We assumed a boom and static ice near the downstream end of the river to generate an ice jam at this location. The river is covered with ice with thickness of 0.25 m at the start of simulation and the ice entering from upstream boundary assumed to be 0.25 m in thickness.

The model successfully applied for this part of the river, the water level through the domain without considering effect of ice cover is shown in Fig. 2b. The final ice thickness and increase in water level due to ice jam is presented in Fig 2c and d. The ice thickness reaches to ~2.7 m at the toe and the water surface elevation difference from downstream to upstream reaches to ~6 m, this is the water surface under the ice cover. Thames River showed ~2.5 m increase in water level at the upstream with the ice jam compare to no ice cover which could result in significant flood threat. The flooding also makes more sediment available for transport which could result in drastic morphological changes.

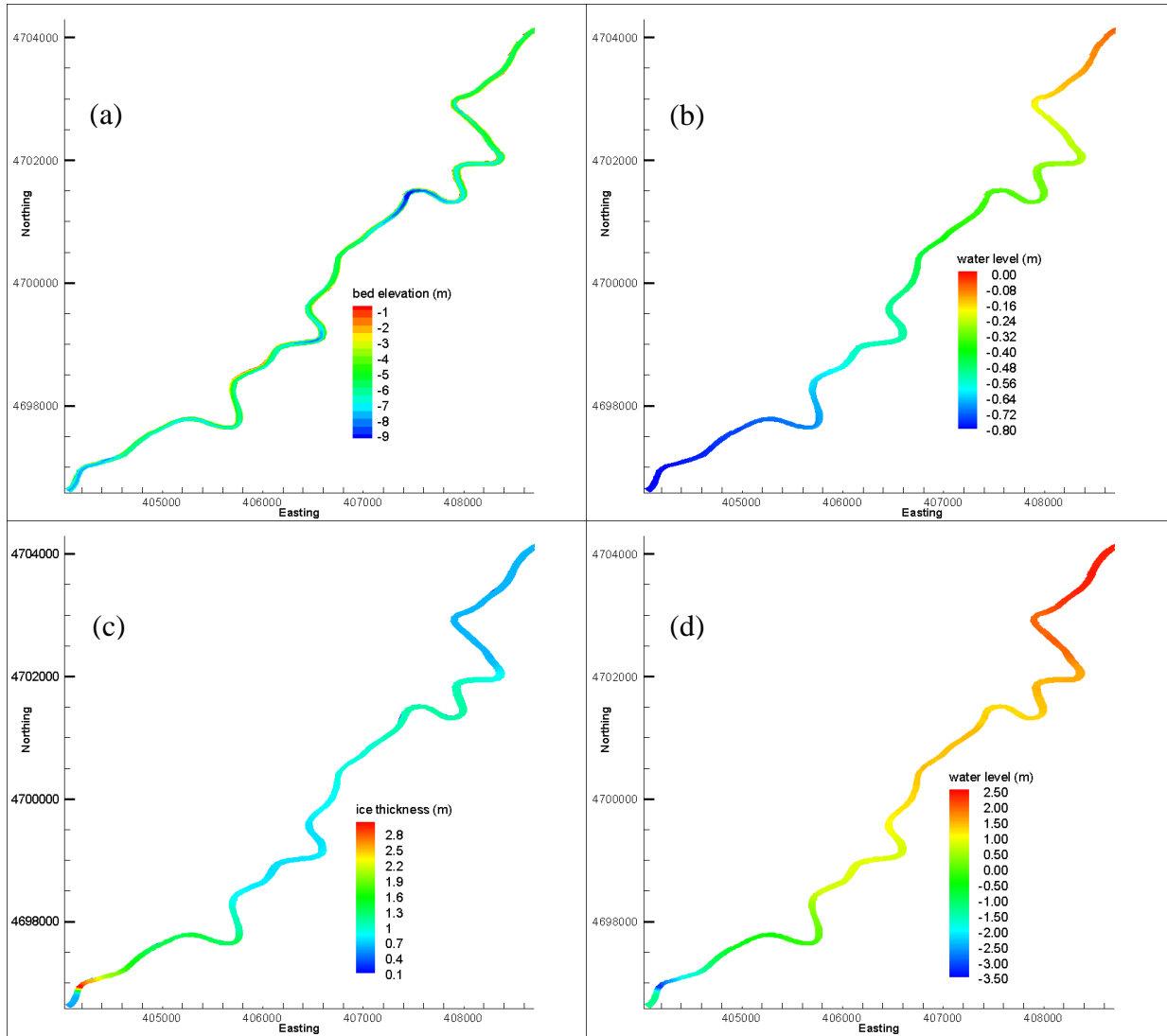


Fig. 2: Thames River model (a) bathymetry, (b) water level without ice, (c) ice thickness after ice jam, (d) water level after ice jam.

8. Conclusion

We presented a discrete parcel method numerical model for modelling of ice dynamic based on MPS. The Lagrangian ice dynamic mode is two-way coupled with Delft3D Eulerian Hydrodynamic model. The ice is assumed to be continuum and the rheology of ice is considered to be viscoplastic. The model solid boundary condition such as river banks is modeled using imaginary particles. The model was successfully agreed with the theory of an idealized static ice jam in rectangular channel. It was also applied on Thames River, ON, Canada to model an ice jam. Although here we do not focus on validation of the code with field data, this will be pursued elsewhere. Here we used a boom to generate the ice jam at specific location therefore it is also shown that the boom boundary condition effectively stops the ice parcels and generate ice jam. This can be used in the location which is known to be potential for ice jam historically or for the location we interested to stop the movement the ice parcels such as hydroelectric dams. Our preliminary analytical testing and application to Thames River indicated the proposed model functionality and applicability in modelling ice dynamic. Also the importance of the modeling ice dynamic in the study of the cold region river is shown. Although this research is focused on ice transport, we plan to include ice formation similar to the one proposed by Oveisy et al. (2014, 2012), to present an integrated ice dynamic and thermodynamic numerical model.

References

- Beltaos, S., 1988. Configuration and Properties of a breakup jam. *Canadian Journal of Civil Engineering*, 15, 685-697.
- Dorsk, A., 2006. Numerical Simulation of Sea Ice Dynamics with the Discrete Element Method. Internal report, Franklin W. Olin College of Engineering.
- Flato, G., 1993. A particle-in-cell sea-ice model. *Atmos. Ocean* 31 (3), 339.
- Goede, E.D, de, Graaff, R.F. de, Wagner, T. and B. Sheets, 2014. Modelling of ice growth and transport on a regional scale, with application to Fountain Lake, Minnesota, USA. OMAE2014-24002.
- Harlow, F. H., 1964. The particle-in-cell computing method for fluid dynamics. *Methods Comput. Phys.* 3 , 319.
- Hibler, W. D., 1979. A dynamic thermodynamic sea ice model. *J. Phys. Oceanogr.* 9, 815.
- Koshizuka S., and Oka, Y., 1996. Moving particle semi-implicit method for fragmentation of incompressible fluid. *Nuclear Science and Engineering*, Vol 123, pp. 421–434, 1996
- Lindsay, R. W., and Stern, H. L., 2004. A new Lagrangian model of Arctic sea ice. *Journal of physical oceanography*. 34(1), 272-283.
- Nolin, S., Roubtsova, V., Morse, B., and Quach, T., 2009. Smoothed particle hydrodynamics hybrid model of ice-jam formation and release. *Canadian Journal of Civil Engineering*. 36(7), 1133-1143.
- Oveisy, A., and Boegman, L., 2014. One-dimensional simulation of lake and ice dynamics during winter. *Journal of Limnology*, 73(3).
- Oveisy, A., Boegman, L., and Imberger, J. 2012. Three-dimensional simulation of lake and ice dynamics during winter. *Limnology and Oceanography*, 57(1), 43-57.
- Pritchard, R. S., Muller, A. C., Hanzlick, D. J. and Yang, Y. S., 1990. Forecasting Bering Sea ice edge behavior. *J. Geophys. Res.* C 95 (1), 775.
- Roubtsova, V., and Kahawita, R., 2009. KIMBULA: A robust 1D model for dambreak and extreme flood simulation. Submitted for publication.

- Shakibaeinia, A., and Jin, Y. C., 2010. A weakly compressible MPS method for simulation open-boundary free-surface flow. *Int. J. Numer. Methods Fluids*, 63(10), 1208–1232.
- Shen, H. T., Gao, L., Kolerski, T., and Liu, L., 2008. Dynamics of ice jam formation and release. *Journal of Coastal Research*, 25-32.
- Shen, H.T., Su, J., and Liu, L., 2000. SPH Simulation of River Ice Dynamics. *J. Computational Physics*, 165, 752-770.
- Shen, H. T., Shen, H. H., and Tsai, S. M., 1990. Dynamic transport of river ice. *J. Hydraul. Res.* 28, 659 (1990).
- Wake, A. and Rumer, R. R., 1983. Great Lakes ice dynamics simulation. *J. Waterway Port Coast. Ocean Eng.* 109, 86.